Int. J. Bio-Inorg. Hybd. Nanomat., Vol. 2, No. 4 (2013), 517-524 *ISSN: 2251-8533*

International Journal of Bio-Inorganic Hybrid Nanomaterials

The Detoxification of Methamidophos as an Organophosphorus Insecticide on the Magnetite (Fe_3O_4) Nanoparticles/Ag-NaY Faujasite Molecular Sieve Zeolite (FMSZ) Composite

Meysam Sadeghi[1*], Mirhassan Hosseini[2]

[1] M.Sc., Young Researchers and Elite Club, Islamic Azad University of Ahvaz Branch, Ahvaz, Iran

[2] M.Sc., Payame Noor University, Germi Moghan, Ardebil, Iran & Nano Center Research, Imam Hossein Comprehensive University (IHCU), Tehran, Iran

Received: 8 October 2013; Accepted: 19 December 2013

ABSTRACT

This work undertakes the study of the detoxification reactions of O, S-dimethyl phosphoramidithioate (methamidophos) as an organophosphorus insecticide on the 14.7 wt% magnetite (Fe_3O_4) nanoparticles/Ag-NaY faujasite molecular sieve zeolite (FMSZ) composite. The influence of solvent (methanol, acetonitrile and n-hexane) on the detoxification potential of composite was investigated. For this survey, in the first step, sodium type-Y (NaY) zeolite was synthesized by hydrothermal method (HM). Then, Ag-NaY zeolite was prepared from NaY zeolite by ion-exchange method (IEM). In the next step, Fe_3O_4 nanoparticles (NPs) were incorporation and deposited on the Ag-NaY zeolite structure by using precipitation method (PM). The synthesized samples were characterized by SEM, EDAX and XRD techniques. The GC-FID and IR analysis results demonstrated that about 99% of methamidophos was detoxified (adsorbed) via this composite at n-hexane solvent after 10 h. On the other hand, the results for the acetonitrile and methanol solvents were lower. It seems that a nonpolar solvent transfer to the reactive surface site on the composite without occupying and blocking of these sites.

Keyword: Detoxification; O, S-dimethyl phosphoramidithioate (methamidophos); Insecticide; magnetite (Fe_3O_4) nanoparticles/Ag-NaY faujasite molecular sieve zeolite (FMSZ); Composite.

1. INTRODUCTION

O, S-dimethyl phosphoramidithioate or methamidophos with molecular formula $C_2H_8NO_2PS$ is an organophosphorus insecticide (Figure 1), poses inevitable threat to persons who make contact, thereby causing health hazards. Its mode of action in insects and mammals is by decreasing the activity of an enzyme important for nervous system function called acetylcholinesterase. This enzyme is essential in the normal transmission of nerve

(*) Corresponding Author - e-mail: meysamsadeghi45@yahoo.com.

impulses. Methamidophos is a potent acetylcholinesterase inhibitor [1, 2]. Recently, there has been growing interest in the development of novel methods and materials for the decontamination and detoxification of organophosphorus pollutants (OPPs). Inorganic metal oxides are well-known for their use in chemical industry as adsorbents, sensors, catalyst, etc. Because of their unique morphological features and high surface area, nanocrystals of metal oxides were used as adsorbents for decomposition or detection of variety of pollutants and harmful substances, including organophosphorous compounds [3]. On the other hand, zeolites are widely used in industry for water and waste water treatment, waste gas treatment, as catalysts, as molecular sieve, in the production of laundry detergents, nuclear processing medicine and in agriculture purposes for the preparation of advanced materials and recently to produce the nanocomposites [4-8]. In a study done via wagner and bartram commercially available NaY and AgY zeolites were used to investigated the reactivity of the actual chemical agents [9]. Zeolites or molecular sieves are crystalline aluminosilicates containing pores and channels of molecular dimensions that are widely used in industry as ion exchange resins, molecular sieves, sorbents and catalysts. A representative empirical formula of a zeolite is: $M_{2/n}.Al_2O_3.ySiO_2.wH_2O$ Where M represents the exchangeable cation of valence n. M is generally a Group I or II ion, although other metal, non-metal and organic cations may also balance the negative charge created by the presence of Al in the structure [10]. Y-zeolite exhibits the FAU (faujasite) structure (Figure 2). It has a 3-dimensional pore structure with

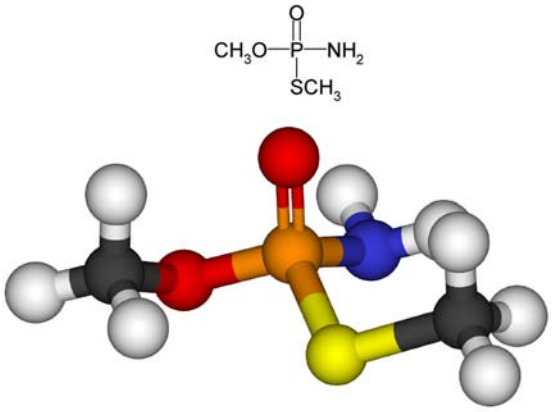

Figure 1: *Structure of O, S-dimethyl phosphoramidithioate (methamidophos).*

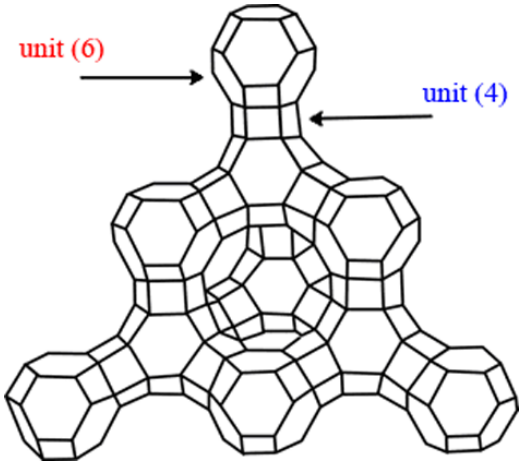

Figure 2: *Structure of type-Y faujasite zeolite.*

pores running perpendicular to each other in the x, y, and z planes similar to LTA, and is made of secondary building units 4, 6, and 6-6 [11, 12].

The methods for modifying zeolites are usually by impregnation [13] and ion-exchange [14]. Iron and its compounds had been important in human life due to its biological and chemical properties. Iron oxides are widespread in earth cortex and play an important role in nature. Recently they have widely utilized in nanocomposite for various application [15-18]. In this research, type-Y zeolite has been selected as the host material for the incorporation of Fe_3O_4 as the guest due to its three dimensional channels which limits the particle size of Fe_3O_4 during the growth. Then, the detoxification studied of methamidophos was carried out by 14.7 wt% magnetite (Fe_3O_4) nanoparticles/Ag-NaY faujasite molecular sieve zeolite (FMSZ) composite at room temperature.

2. EXPERIMENTAL

All chemical are purchased from Merck and Alfa Aesar German Fluka was used as received.

2.1. Preparation of NaY zeolite by hydrothermal method (HM)

At first, 10 g of sodium hydroxide was mixed with 10 mL of distilled water until being dissolved. 9.75 g of alumimium trihydrate was dissolved in the sodium hydroxide solution which was previously heated to 100°C. 10 g of the prepared solution was mixed

with 61.2 mL of distilled water and 5.9 g of sodium hydroxide until being dissolved (solution A). The solution of 22 g of sodium silicate was slowly added to the solution containing 5.9 g of sodium hydroxide and 61.2 ml of distilled water, then, were mixed until being dissolved (solution B). Solution A was slowly added to solution B and mixture was well agitated for 30 min. The solution was transferred to a stainless steel autoclave lined with PTFE (Teflon) and kept in a static air oven at 90°C for 8 h. The crystalline material was separated by filtration and washed with distilled water until the pH was neutral (pH= 8). Finally, the materials were dried at 100°C [19].

2.2. Preparation of Ag-NaY zeolite by ion exchange method (IEM)

In a typical preparation procedure, 2 g of the synthesized NaY zeolite calcined at 400°C for 2 h. The calcined NaY zeolite was then added to a 50 mL of a 0.15 M silver nitrate ($AgNO_3$) solution and the mixture was stirred at 60°C for 5 h to perform ion exchange process. The resulting zeolite was filtered and washed with deionized water, then dried at 110°C for 16 h. Finally, the clean and dry zeolite was calcined in a furnace for 4 h at 400°C [20].

2.3. Preparation of Fe_3O_4 nanoparticles/Ag-NaY zeolite composite by precipitation method (PM)

For the synthesis of Fe_3O_4 nanoparticles/Ag-NaY zeolite composite, at first 1.5 g of Ag-NaY zeolite was added to 40 mL of distilled water and slowly stirs for 10 min until homogenate suspension was obtained. After that a desired quantity of $FeCl_3$ and $FeCl_2$ solutions with molar ratio of 2:1 was added into the suspension and stir for 30 min. Then while the mixture was being stirred vigorously about 20 mL of 1 M NaOH solution was slowly added and vigorous stirring was continued for another 30 min. The synthesized product (Fe_3O_4 nanoparticles/Ag-NaY zeolite) was then filtered, washed with distilled water and finally dried in oven at 50°C [13].

2.4. Reaction procedure of Fe_3O_4 nanoparticles/Ag-NaY zeolite composite with methamidophos (composite/methamidophos sample)

For the investigation of the reaction between Fe_3O_4 nanoparticles/Ag-NaY zeolite composite and methamidophos. the samples were prepared according to the following method: 5 mL of methanol, acetonitrile or n-hexane as the solvent, 10 μL of methamidophos, 10 μL of octane as internal standard and 0.35 g of Fe_3O_4 nanoparticles/Ag-NaY zeolite composite were added to the 100 mL Erlenmeyer flask. To do a complete reaction between composite and organophosphorus compound, all samples were attached to a shaker and were shaken for 10 h under N_2 atmosphere and in room temperature. Then, by micropipette extracted 1 μL of solution and injected to GC instrument.

2.5. Characterization of samples

The morphology and particle size of the crystalline zeolites and composite were analyzed using SEM images. Semiquantitative analysis were carried out on an energy-dispersive x-ray spectrometer (EDAX) connected to LEO-1530VP XL30 Philips scanning electron microscope. Prior to the measurement, the samples were coated with a thin layer of gold. Powder X-ray diffraction (XRD) patterns were recorded at room temperature using a Philips X'Pert Pro Diffractometer with Ge-monochromated Cu-Kα1 radiation with a wavelength of 1.54056 Å. Data were collected over the range 4-90° in 2θ with a scanning speed of 2°/min.

The GC-FID and was used for the detoxification reactions. A Varian Star 3400CX series gas chromatograph equipped with flame ionization detector (FID) and an OV-101CWHP 80/100 silica capillary column (30 m × 0.25 mm inner diameter (i.d), 0.25 μm film thickness) was used to monitor the decontamination reactions. The GC conditions used were as follows: the column temperature was initially hold at 60°C for 6 min and programmed at 20°C min^{-1} to 200°C to reach the final temperature which was then held for 13 min.

The injector, MS quad and source temperatures were fixed at 60°C, 200°C and 230°C, respectively. Helium (99.999 % purity) was selected as the carrier gas with the flow rate of 1 mL min^{-1}. The IR spectrum was scanned using a Perkin-Elmer FTIR (Model 2000) in the wavelength range of 450 to 4000 cm^{-1} with KBr pellets method.

3. RESULT AND DISCUSSION

3.1. Scanning electron microscope (SEM) study

The morphology and crystallite size of the as-synthesized samples were investigated by SEM images (Figure 1). Comparison between the morphologies of Na-Y and Ag-NaY zeolites shows that the cubic morphology and crystalline size are retained with ion exchange and were in the regions of the micro-scale (Figure 3a and 3b). On the other hand, as it is indicated by image with high resolution, the Fe_3O_4 nanoparticles have appeared and deposited on the external surface of Ag-NaY zeolite (Figure 3c). The crystallite size for the Fe_3O_4 nanoparticles was less than 100 nm. Also, some particles aggregation has occurred due to synthesize of nanoparticles of Fe_3O_4 on the surface of zeolite.

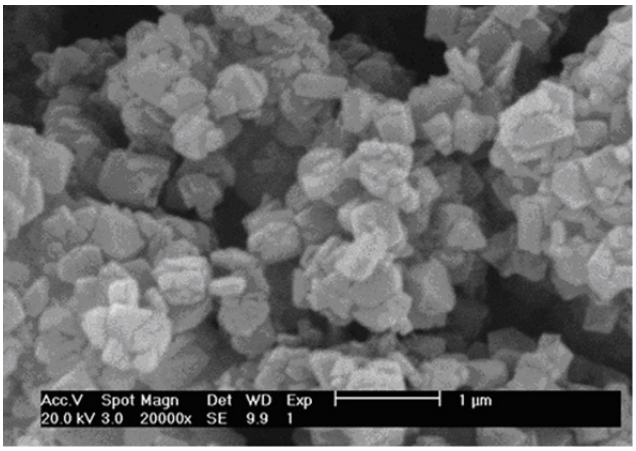

(a)

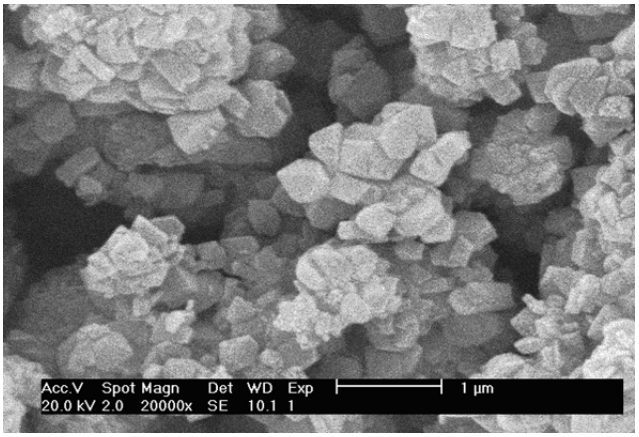

(b)

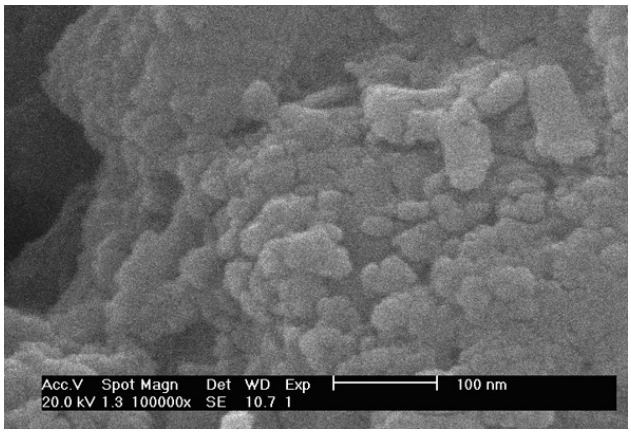

(c)

Figure 3: *The SEM images of the samples: (a) NaY, (b) Ag-NaY, c) 14.7 wt% Fe_3O_4 nanoparticles/Ag-NaY.*

3.2. Energy-dispersive x-ray spectrometer (EDAX) analysis

Figure 4 give the composition elements present in Fe_3O_4 nanoparticles/Ag-NaY zeolite composite was investigated by energy dispersive X-rays (EDAX) analysis. In the EDAX spectrum of composite, the appeared peaks in the regions of approximately 0.55, 1.05, 1.50, 1.75 and 2.92 and 3.21 keV are corresponded to the binding energies of oxygen (O), sodium (Na), aluminum (Al), silicon (Si) and silver (Ag) respectively that are related to the Ag-NaY zeolite. On the other hand, in this spectrum, the appeared two peaks in the regions of 6.23 and 6.94 keV are related to the binding energies of iron (Fe) which reveals the presence of Fe in the composite. These results confirm coexistence of 18.3 wt% and 14.7 wt% silver and iron in the prepared sample, respectively.

3.3. X-Ray diffraction (XRD) patterns

The XRD patterns of the synthesized NaY and Ag-NaY zeolites and 14.7 wt% Fe_3O_4 nanoparticles/

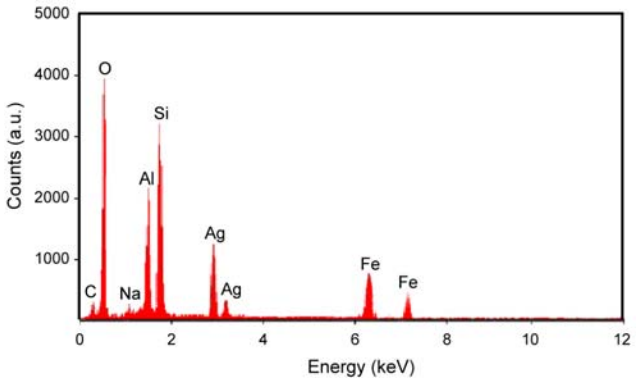

Figure 4: *The EDAX analysis of the 14.7 wt% Fe_3O_4 nanoparticles/Ag-NaY.*

Ag-NaY zeolite composite under study are shown in Figure 5. The structure of the NaY zeolite was retained after the silver-cation exchanges (Figure 5a and 5b). However, for Ag-NaY zeolite, a small loss of crystallinity is observed, associated with the lower intensity of the peaks at 2Theta=10-34. This effect could be related to a dealumination of its structure, possibly associated with the location of extra-framework silver. Also, XRD patterns showed that the Ag-NaY zeolite and Fe_3O_4 nanoparticles/Ag-NaY are almost similar to the parent (NaY zeolite). The 14.7 wt% Fe_3O_4 deposited in the pores of Ag-NaY zeolite does show a series new diffraction peak. The peaks of Fe_3O_4 phase appeared at 2θ values of 36.34°, 43.54°, 59.38°, 61.75° and 74.32° corresponding to the diffraction planes (D311), (D400), (D511), (D440) and (D662), respectively [13, 21]. These peaks are illustrated as the red points in Figure 5c. The structures of prepared Fe_3O_4 nanoparticles deposited in the Ag-NaY zeolite were investigated via X-ray diffraction (XRD) measurement. The average particle size was calculated from line broadening of the peak at 2θ=4-90° using Debye-Scherrer equation:

$$d = \frac{0.94\lambda}{\beta \cos\theta} \quad (1)$$

Where d is the crystalline size, λ is the wavelength of X-ray source, β is the full width at half maximum (FWHM) and θ is the angle of incidence for the selected diffraction peak (Bragg diffraction angle). The average crystallite size of the Fe_3O_4 nanoparticles were calculated about 31 nm.

3.4. GC-FID analysis

The detoxification (adsorption/destruction) reactions between 14.7 wt% Fe_3O_4 nanoparticles/Ag-NaY zeolite composite and methamidophos was investigated and monitored by GC-FID. To accede maximum efficiency, the effects of different solvents and time intervals have been investigated. The GC chromatograms, area under curve (AUC) data and results under different conditions are summarized in Figures 6 and 7 and Table 1. To calculate the amounts of detoxified organo-phosphorous insecticide, the integrated area under peak data of two samples, methamidophos and octane as the internal standard have been given for all solvents and times. Subsequently, the ratios of the integrated data (integrated AUC of methamidophos/integrated AUC of octane) were determined. The experiments were performed at different time intervals from 0 and 10 h. With increasing the time, AUC amounts of methamidophos were firstly decreased until 10 h, and then a slight increasing trend was observed. These results confirm that the composite is perfectly able to de-

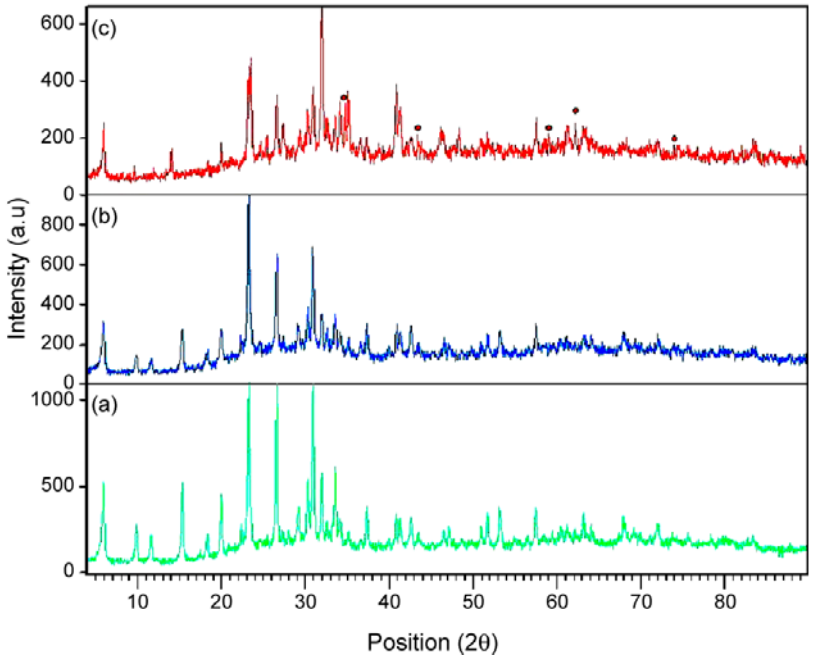

Figure 5: *The XRD patterns of the samples, (a) Na-Y, (b) Ag-NaY, c) Fe_3O_4 nanoparticles/Ag-NaY.*

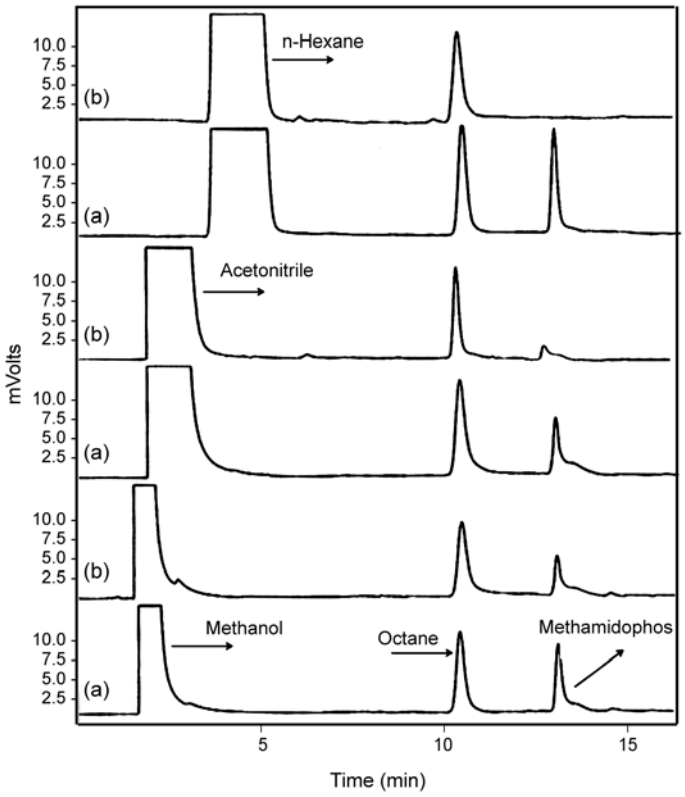

Figure 6: *The GC chromatograms for methamidophos-Fe3O4 nanoparticles/Ag-NaY sample.*

toxification methamidophos (99%) at n-hexane after 10 h. On the other hand, the detoxification data were lower for acetonitrile and methanol as the solvents. Notwithstanding the transition state must be involved in the polar reaction, polar solvent hinders the reaction's progress.

It could be construed from GC analysis that polar solvent can compete with the reaction sites presented on the surface of the composite including Bronsted (hydroxyl groups (Fe-OH)) and Lewis acid (Fe^{3+}) sites. In particular, the blocking of Lewis acid sites would hinder the coordination of methamidophos. Since methanol is considered as such a strong hindrance to the reaction, this points out to the fact that isopropanol simply blocks access to the surface of the catalyst.

3.5. FT-IR spectrum

The FT-IR spectrum of the 14.7 wt% Fe_3O_4 nanoparticles/Ag-NaY zeolite composite after the reaction

Table 1: *The GC analysis results in the presence of different solvents, (a) zero time (the blank solution) and (b) after 10 h.*

Solvent	Sample	AUC/Octane (1)	AUC/ methamidophos (2)	Ratio (AUC 2/AUC 1)	Detoxified (%)
Methanol	a	356489	333567	0.9357	100.00
	b	356246	234605	0.6581	70.34
Acetonitrile	a	397726	332461	0.8359	100.00
	b	373228	131568	0.3308	39.58
n-Hexane	a	410687	405992	0.9885	100.00
	b	395247	000000	000000	00.00

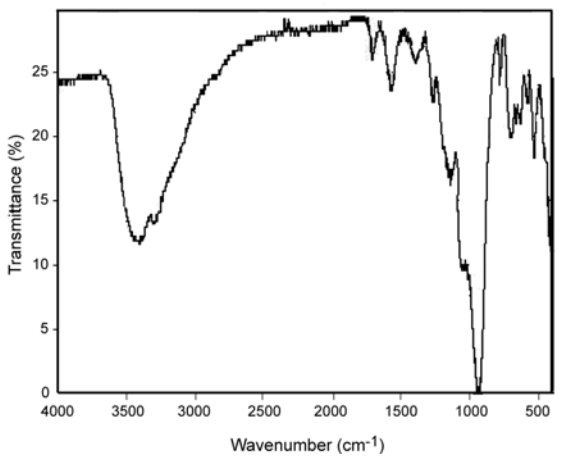

Figure 7: *The IR spectrum for adsorbed O, S-dimethyl phosphoramidithioate (methamodophos) on the 14.7 wt% Fe_3O_4 nanoparticles/Ag-NaY zeolite composite.*

with methamidophos is shown in Figure 7. The peak at 463 cm^{-1} is corresponded to the structure insensitive internal TO_4 (T= Si or Al) tetrahedral bending peak of Y-zeolite. The peak at 562 cm^{-1} is attributed to the double ring external linkage peak assigned to Y-zeolite. The peaks at 676 and 754 cm^{-1} are assigned to external linkage symmetrical stretching and internal tetrahedral symmetrical stretching respectively (D6R). Furthermore, the peaks at 988 cm^{-1} and 1070 cm^{-1} are assigned to internal tetrahedral asymmetrical stretching and external linkage asymmetrical stretching respectively and peaks around 1638 and 3480 cm^{-1} are assigned to H-O-H bending and hydroxyl groups of the zeolite, respectively. Also, the new peaks at 3429 (H-O-H), 1437 (C-C) and 578 (Fe-O) cm^{-1} regions are corresponded to the synthesized Fe_3O_4 nanoparticles. On the other hand, the adsorption of methamidophos on the 14.7 wt% Fe_3O_4 nanoparticles/Ag-NaY zeolite was investigated by IR spectrum. The new peaks at 1732, 1354, 1238 and 862 cm^{-1} are seen. These observed IR data lead to an understanding of the adsorption reaction of methamidophos on the surface of composite (Figure 8).

4. CONCLUSIONS

In this paper, NaY and Ag-NaY zeolites were synthesized by hydrothermal and ion-exchange methods, respectively. In the next step, 14.7 wt% Fe_3O_4 nanoparticles/zeolite Ag-NaY composite was prepared using precipitation method. The detoxification (adsorption) of methamidophos on this composite was investigated. The results emphasized that about 99% of methamidophos molecule was adsorbed at n-hexane solvent after 10 h.

ACKNOWLEDGEMENTS

The authors gratefully acknowledge the financial supports of Tehran Imam Hossein comprehensive University (IHCU), Iran.

REFERENCES

1. Antonious G.F., Snyder J.C., *Bull. Environ. Contam. Toxicol*, **52** (1994), 141.
2. Hussain M.A., *Bull. Environ. Contam. Toxicol*, **38** (1987), 131.
3. Richards R., Li W., Decker S., Davidson C. et al., *J. Am. Chem. Soc.*, **122** (2000), 4921.
4. Nedeljkovic D.M., Stajcic A.P., Dig A.S. et al., *J. Nanomater. Bios*, **7** (2012), 269.
5. Al-Matar H.M., Khalil K.D., Al-Kanderi M.F., Elnagdi M.H., *Molecules*, **17** (2012), 897.
6. Ibrahim H.M., Behbehani H., Makhseed S., Elnagdi M.H., *Molecules*, **16** (2011), 3723.
7. Batista A.C.L., Villanueva E.R., Amorim R.S., Tavares M.T., Campos-Takaki G.M., *Molecules*, **16** (2011), 3569.
8. Okumura K., Tomiyama T., Moriyama S., Nakamichi A., Niwa M., *Molecules*, **16** (2000), 38.
9. Wagner G.W., Bartram P.W., *Langmuir*, **15** (1999), 8113.
10. Cundy C.S., *Stud. Surf. Sci. Catal.*, **57** (2005), 65.
11. C.H. Barlocher, W.M. Meier, D.H. Olson, 2001. *Atlas of Zeolite Structure Types*, 5th edn. Elsevier.
12. Ghobarkar H., Schlaf O., Guth U., *Prog. Solid. St. Chem.*, **27** (1999), 29.
13. Jahangirian H. et al., *Dig. J. Nanomater. Bios*, **8** (2013), 1405.
14. Yamamoto T., Apiluck E., Kim S., Ohmori T., *J. Ind. Eng. Chem.*, **13** (2007), 1142.
15. Wang Z., Cuschieri A., *Int. J. Mol. Sci.*, **14** (2013), 9111.

16. Khandanlou R., Ahmad M., Shameli K., Kalantari K., *Molecules*, **18** (2013), 6597.
17. Granitzer P., Rumpf K., *Materials*, **4** (2011), 908.
18. Iconaru S.L., Andronescu E., Ciobanu C.S., Prodan A.M., Coustumer P. L, Predoi D., *Dig. J. Nanomater. Bios*, **7** (2012), 399.
19. Elliott C.H., McDaniel C.V., *US Pat.* No. **3** (1970), 639.
20. Kim S.O., Park E.D., Ko E.Y., *US Pat.* No. **25** (2006), 57.
21. Ghandoor H.E., Zidan H.M., Mostafa M.H., Ismail I.M., *Int. J. Electrochem. Sci.*, 7 (2012), 5734.